

Lattice Dynamics of White Tin

T. WOLFRAM, G. W. LEHMAN, AND R. E. DE WAMES

North American Aviation Science Center, Canoga Park, California

(Received 15 November 1962)

The theoretical lattice vibrational spectrum for white tin (body-centered tetragonal) is examined on the basis of the axially symmetric lattice dynamics model including fourth-nearest-neighbor interactions. The atomic force constants are derived using experimental data for the elastic constants, specific heat, Debye temperature, and the Debye-Waller factor at 100°K. The 6×6 dynamical matrix is diagonalized along the principal symmetry directions and the resulting dispersion curves are presented. The spectrum is characterized by low-lying optical modes which interact strongly with the acoustic modes, particularly near the surface of the first Brillouin zone. These optical modes give rise to a large density of states at intermediate acoustical frequencies and contribute significantly to both the specific heat and Debye-Waller factor at low temperature.

I. INTRODUCTION

A CONSIDERABLE amount of experimental and theoretical work has been devoted to the study of Mössbauer and superconducting properties of white tin. However, no investigation of the detailed nature of its lattice vibrations has yet been made.¹

Our principal motivation for examining the theoretical vibrational spectrum of white tin was to determine its lattice dispersion and polarization vectors which are prerequisites for the calculation of the Debye-Waller factor occurring in the Mössbauer theory. The results of this calculation will be presented in a subsequent paper.² Furthermore, it is of considerable interest to apply the axially symmetric lattice dynamics model (A-S model) recently developed and used with success in the study of the vibrational spectrum of copper and aluminum.³ In addition, it is hoped that this work may stimulate an effort to observe the spectrum of white tin experimentally.

White tin is a particularly interesting crystal to study because it possesses optical modes and because it is non-cubic. The specific heat rises very rapidly at low temperatures indicating that the optical branches are rather low lying. This conjecture is also supported by the large Debye-Waller factor possessed by white tin at low temperatures. The tetragonal structure gives rise to a directionally dependent Debye-Waller factor,^{2,4} $2W$.

Although there is no direct experimental data on the dispersion in tin, there is sufficient physical data relating to the lattice vibrations so that a reasonably accurate picture of the phonon spectrum can be constructed.

In Sec. II, we give a discussion of the form of the dynamical matrix for body-centered tetragonal white tin based on the A-S model. The dynamical matrix is block diagonalized along the various symmetry directions. In Sec. III, the dynamical matrix is separated into

an acoustic and an optical matrix near the center of the Brillouin zone by transforming to the center-of-mass system. The optical frequencies at the center of the zone are obtained. The acoustic portion of the dynamical matrix is correlated with the elastic constants in Sec. IV, and the atomic-force constants evaluated. Section V is concerned with the results and a discussion of our study. The dispersion curves and specific-heat calculations are also presented. In Appendix A, we show that the stability conditions for the white tin lattice are automatically satisfied by the A-S model and in Appendix B the A-S model is discussed briefly. The matrix elements for white tin are given in Appendix C.

II. DYNAMICAL MATRIX

The structure of white tin may be described as two interpenetrating body-centered tetragonal lattices. Sublattice one is centered at (0,0,0) and the second sublattice is centered at (0, $a/2$, $c/4$). The lattice constants are $a = 5.82 \text{ \AA}$ and $c = 3.18 \text{ \AA}$. This gives an a/c ratio of 1.83. The atomic structure is shown in Fig. 1(a). The first Brillouin zone is a truncated rectangular parallelepiped as shown in Fig. 1(b). The two inequivalent lattice sites give rise to six vibrational branches. In the long-wavelength limit three of these branches can be described as optical and three as acoustic.

A discussion of the A-S lattice dynamics model is given in Appendix A and the resulting matrix elements for white tin are derived in Appendix B. The following analysis is applicable to any crystal with tetragonal symmetry and two inequivalent lattice sites. The form of the dynamical matrix is

$$\mathfrak{D}(\mathbf{q}) = \begin{bmatrix} D_{11}(\mathbf{q}) & D_{12}(\mathbf{q}) \\ D_{12}(\mathbf{q})^* & D_{11}(\mathbf{q}) \end{bmatrix}. \quad (1)$$

Here, \mathbf{q} denotes a vector in the first Brillouin zone and the elements, $D_{\alpha\beta}(\mathbf{q})$, of the above 2×2 supermatrix are 3×3 matrices. $\mathfrak{D}(\mathbf{q})$ can be transformed to a real form by the unitary transformation

$$U = \frac{1}{\sqrt{2}} \begin{bmatrix} I & iI \\ -iI & I \end{bmatrix}. \quad (2)$$

¹ Phillips has made a study of the vibrational spectrum in gray (diamond structure) tin; however, the dispersion curves were not derived. J. C. Phillips, *Phys. Rev.* **113**, 147 (1959).

² R. De Wames, T. Wolfram, and G. W. Lehman (to be published); see also *Bull. Am. Phys. Soc.* **7**, 500 (1962).

³ G. W. Lehman, T. Wolfram, and R. E. De Wames, *Phys. Rev.* **128**, 1593 (1962).

⁴ Y. Kagen, *Dokl. Akad. Nauk. S.S.S.R.* **40**, 794 (1961).

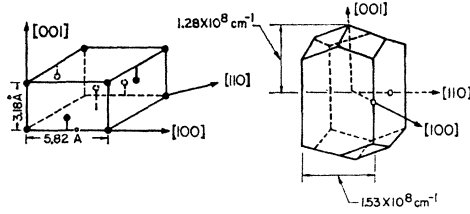


FIG. 1. Atomic unit cell and Brillouin zone for white tin.

where I is a 3×3 unit matrix. Thus, for the transformed dynamical matrix $L(\mathbf{q})$, we obtain

$$L(\mathbf{q}) = U^* \mathfrak{D}(\mathbf{q}) U = \begin{bmatrix} (D_{11} + \text{Im}D_{12}) & \text{Re}D_{12} \\ \text{Re}D_{12} & (D_{11} - \text{Im}D_{12}) \end{bmatrix}, \quad (3)$$

where $\text{Re}D_{12}$ and $\text{Im}D_{12}$ denote the real and imaginary part of the matrix D_{12} . In terms of a 6×6 matrix, $L(\mathbf{q})$ may be written as

$$L(\mathbf{q}) = \begin{pmatrix} d_{11} & d_{12} & d_{13} & \cdots & d_{16} \\ d_{21} & d_{22} & d_{23} & \cdots & d_{26} \\ \vdots & \vdots & \vdots & \ddots & \vdots \\ d_{61} & d_{62} & d_{63} & \cdots & d_{66} \end{pmatrix}. \quad (4)$$

The correspondence between the d 's and the matrices $D_{\alpha\beta}$ is obvious. For example,

$$(D_{11} + \text{Im}D_{12}) = \begin{pmatrix} d_{11} & d_{12} & d_{13} \\ d_{21} & d_{22} & d_{23} \\ d_{31} & d_{32} & d_{33} \end{pmatrix}. \quad (5)$$

The white-tin structure possesses a screw axis so that it is necessary to consider the space group to work out all of the details of a group theoretical analysis. It is sufficient, however, to consider only the point group of the points in the Brillouin zone in order to obtain the degeneracies associated with the acoustic modes. The group of the q vector along the $[100]$ and $[110]$ directions is C_{2v} , and along the $[001]$ it is C_{4v} . Only the group C_{4v} possesses a two-dimensional irreducible representation and, consequently, the transverse acoustic branches are required to be doubly degenerate only along the $[001]$ direction.

Using group theoretical arguments, one can block diagonalize the dynamical matrix along the principal symmetry directions. For example, along the $[100]$ direction in the Brillouin zone the block diagonalized dynamical matrix L' is

$$L'(\mathbf{q} = (x0,0)) = \begin{pmatrix} d_{11} & d_{16} & 0 & 0 & 0 & 0 \\ d_{16} & d_{66} & 0 & 0 & 0 & 0 \\ 0 & 0 & d_{33} & d_{34} & 0 & 0 \\ 0 & 0 & d_{34} & d_{44} & 0 & 0 \\ 0 & 0 & 0 & 0 & d_{22} & 0 \\ 0 & 0 & 0 & 0 & 0 & d_{55} \end{pmatrix}. \quad (6)$$

The acoustic frequencies are

$$\omega_{3L}^2 = \frac{1}{2} \{ (d_{11} + d_{66}) - [(d_{11} + d_{66})^2 - 4(d_{11}d_{66} - d_{16}^2)]^{1/2} \},$$

$$\omega_{2T}^2 = d_{22}, \quad (7)$$

$$\omega_{1T}^2 = \frac{1}{2} \{ (d_{33} + d_{44}) - [(d_{33} + d_{44})^2 - 4(d_{33}d_{44} - d_{34}^2)]^{1/2} \},$$

where T and L denote transverse and longitudinal in the usual sense. The elements d_{ij} are evaluated at $\mathbf{q} = (x,0,0)$. The optical frequencies are

$$\omega_{40}^2 = \frac{1}{2} \{ (d_{11} + d_{66}) + [(d_{11} + d_{66})^2 - 4(d_{11}d_{66} - d_{16}^2)]^{1/2} \},$$

$$\omega_{50}^2 = \frac{1}{2} \{ (d_{33} + d_{44}) + [(d_{33} + d_{44})^2 - 4(d_{33}d_{44} - d_{34}^2)]^{1/2} \}, \quad (8)$$

$$\omega_{60}^2 = d_{55}.$$

Similarly, for elastic waves propagating along the $[001]$ direction,

$$L'(\mathbf{q} = (0,0,x)) = \begin{pmatrix} d_{11} & d_{14} & 0 & 0 & 0 & 0 \\ d_{14} & d_{44} & 0 & 0 & 0 & 0 \\ 0 & 0 & d_{22} & d_{25} & 0 & 0 \\ 0 & 0 & d_{25} & d_{55} & 0 & 0 \\ 0 & 0 & 0 & 0 & d_{33} & 0 \\ 0 & 0 & 0 & 0 & 0 & d_{66} \end{pmatrix}, \quad (9)$$

with acoustic frequencies

$$\omega_{1T}^2 = \frac{1}{2} \{ (d_{11} + d_{44}) - [(d_{11} + d_{44})^2 - 4(d_{11}d_{44} - d_{14}^2)]^{1/2} \},$$

$$\omega_{2T}^2 = \omega_{1T}^2, \quad d_{14} = d_{25}, \quad d_{11} = d_{22}, \quad d_{44} = d_{55}, \quad (10)$$

$$\omega_{3L}^2 = d_{33},$$

and optical frequencies,

$$\omega_{40}^2 = \frac{1}{2} \{ (d_{11} + d_{44}) + [(d_{11} + d_{44})^2 - 4(d_{11}d_{44} - d_{14}^2)]^{1/2} \},$$

$$\omega_{50}^2 = \omega_{40}^2, \quad (11)$$

$$\omega_{60}^2 = d_{66}.$$

Along the $[110]$ direction in the Brillouin zone, the dynamical matrix breaks up into two 3×3 matrices:

$$L'(\mathbf{q} = (x,x,0)) = \begin{pmatrix} d_{11} & d_{12} & d_{16} & 0 & 0 & 0 \\ d_{12} & d_{11} & d_{26} & 0 & 0 & 0 \\ d_{16} & d_{26} & d_{66} & 0 & 0 & 0 \\ 0 & 0 & 0 & d_{44} & d_{45} & d_{34} \\ 0 & 0 & 0 & d_{45} & d_{44} & d_{35} \\ 0 & 0 & 0 & d_{34} & d_{35} & d_{33} \end{pmatrix}, \quad (12)$$

and the frequencies are the roots of the following cubic equations:

$$\omega_6^2 + \alpha_i \omega^4 + \beta_i \omega^2 + \gamma_i = 0 \quad (i=1, 2), \quad (13)$$

where

$$\alpha_1 = -2d_{11} + d_{66},$$

$$\beta_1 = -d_{11}^2 + 2d_{11}d_{66} - d_{26}^2 - d_{12}^2 - d_{16}^2, \quad (14)$$

$$\gamma_1 = -d_{26}^2 d_{11} - d_{11}^2 d_{66} + d_{12}^2 d_{66} + d_{16}^2 d_{11} - 2d_{12} d_{16} d_{26},$$

and

$$\alpha_2 = -2d_{44} + d_{33},$$

$$\beta_2 = -d_{44}^2 + 2d_{44}d_{33} - d_{35}^2 - d_{45}^2 - d_{34}^2, \quad (15)$$

$$\gamma_2 = -d_{35}^2 d_{44} - d_{44}^2 d_{33} + d_{45}^2 d_{33} + d_{34}^2 d_{44} - 2d_{45} d_{34} d_{35}.$$

III. CENTER-OF-MASS SYSTEM

In the long-wavelength limit, each sublattice moves as a unit either in phase (acoustic modes) or 180° out of phase (optical modes). In the center-of-mass system, the “in-phase” motions of the two sublattices will have zero frequencies, while the “out-of-phase” motions will have nonzero frequencies. Since these two motions are orthogonal, the dynamical matrix will be block diagonal with two 3×3 matrices down the diagonal. One matrix will have three roots which vanish as $\mathbf{q} \rightarrow (0,0,0) \equiv \mathbf{0}$ and corresponds to the acoustic matrix that one obtains from elastic theory. The second matrix has three roots which do not vanish as $\mathbf{q} \rightarrow \mathbf{0}$. These roots are the optical frequencies. This block diagonalization is accomplished by transforming the dynamical matrix, $\mathfrak{D}(\mathbf{q})$, to the center-of-mass system by means of the unitary supermatrix V ,

$$V = \frac{1}{\sqrt{2}} \begin{bmatrix} I & I \\ -I & I \end{bmatrix}. \tag{16}$$

The dynamical matrix in the center-of-mass system is

$$\Lambda(\mathbf{q}) = V^* \mathfrak{D}(\mathbf{q}) V = \begin{bmatrix} (D_{11} + \text{Re}D_{12}) & -\text{Im}D_{12} \\ -\text{Im}D_{12} & (D_{11} - \text{Re}D_{12}) \end{bmatrix}. \tag{17}$$

Since the dynamical matrix $\mathfrak{D}(\mathbf{q}=\mathbf{0})$ must be real, we have $\text{Im}D_{12}(\mathbf{q}=\mathbf{0})=0$. Furthermore, from the definition of $D_{11}(\mathbf{q})$ given by (B4), it is apparent that

$$D_{11}(\mathbf{0}) = -\text{Re}D_{12}(\mathbf{0}). \tag{18}$$

Therefore, $\Lambda(\mathbf{0})$ is block diagonal. The matrix $G(\mathbf{q}) = (D_{11} + \text{Re}D_{12})$ vanishes at $\mathbf{q}=\mathbf{0}$ and, therefore, corresponds to the acoustic matrix in the long-wavelength limit. The optical frequencies for small propagation vectors are determined by the matrix $(D_{11} - \text{Re}D_{12})$. Group theoretical arguments show that the three optical frequencies at the center of the Brillouin zone consist of a twofold degenerate root ω_a and a singly degenerate frequency ω_b .

It is easily seen from the dynamical matrix elements given in Appendix B that

$$(D_{11} - \text{Re}D_{12})|_{\mathbf{q}=\mathbf{0}} = 2D_{11}(\mathbf{0}) = \begin{bmatrix} \omega_a^2 & 0 & 0 \\ 0 & \omega_a^2 & 0 \\ 0 & 0 & \omega_b^2 \end{bmatrix}, \tag{19}$$

where

$$\omega_b^2 = \frac{2}{m} \{ 4C_2(1,12) + 8\gamma^2 \delta_2 k_1(1,12) + 8\gamma^2 \delta_3 k_1(3,12) + 4C_2(3,12) \}, \tag{20}$$

and

$$\omega_a^2 = \frac{2}{m} \{ 4C_2(1,12) + 4\delta_2 k_1(1,12) + 36\delta_3 k_1(3,12) + 4C_2(3,12) \}. \tag{21}$$

The constant γ is the a/c ratio and

$$\delta_1 = \frac{1}{2\gamma^2 + 1}, \quad \delta_2 = \frac{1}{4\gamma^2 + 1}, \quad \delta_3 = \frac{1}{4\gamma^2 + 9}. \tag{22}$$

The $C(s,\alpha\beta)$ and $K(s,\alpha\beta)$ are atomic force constants defined in Appendix B.

It is important to note that only the atomic force constants which refer to interactions between the two sublattices, $(\alpha\beta=12)$, are involved in the optical frequencies. This is because in these optical modes each sublattice moves as a unit with the two sublattices 180° out of phase. The centroid of the square of the optical frequencies, ω_{av}^2 , is independent of γ and is defined by

$$\omega_{av}^2 = \frac{1}{3} [2\omega_a^2 + \omega_b^2] = \frac{8}{m} [C_2(1,12) + C_2(3,12) + \frac{1}{3} k_1(1,12) + k_1(3,12)]. \tag{23}$$

IV. ELASTIC EQUATIONS AND ATOMIC FORCE CONSTANTS

According to elastic theory, the dynamical matrix, $E(\mathbf{q})$, for the acoustic modes of a crystal with tetragonal symmetry is⁵

$$\rho E(\mathbf{q}) = \begin{bmatrix} C_{11}q_x^2 + C_{66}q_y^2 + C_{44}q_z^2 & (C_{12} + C_{66})q_x q_y & (C_{13} + C_{44})q_x q_z \\ (C_{12} + C_{66})q_x q_y & C_{66}q_x^2 + C_{11}q_y^2 + C_{44}q_z^2 & (C_{13} + C_{44})q_y q_z \\ (C_{13} + C_{44})q_x q_z & (C_{13} + C_{44})q_y q_z & C_{44}(q_x^2 + q_y^2) + C_{33}q_z^2 \end{bmatrix}, \tag{24}$$

where ρ is the density, q_α is the α th Cartesian component of the propagation vector and the C_{ij} are the elastic constants. The frequencies are determined by the secular equation

$$|E(\mathbf{q}) - \omega^2 I| = 0. \tag{25}$$

Along the [100] direction, the frequencies are

$$\begin{aligned} \rho\omega_{1T}^2 &= C_{44}q^2, \\ \rho\omega_{2T}^2 &= C_{66}q^2, \\ \rho\omega_{3L}^2 &= C_{11}q^2. \end{aligned} \tag{26}$$

The frequencies for elastic waves propagating along the [001] are

$$\begin{aligned} \rho\omega_{1T}^2 &= C_{44}q^2, \\ \rho\omega_{2T}^2 &= C_{44}q^2, \\ \rho\omega_{3L}^2 &= C_{33}q^2; \end{aligned} \tag{27}$$

and along the [110],

$$\begin{aligned} \rho\omega_{1T}^2 &= C_{44}q^2, \\ 2\rho\omega_{2T}^2 &= (C_{11} - C_{12})q^2, \\ 2\rho\omega_{3L}^2 &= (C_{11} + C_{12} + 2C_{66})q^2. \end{aligned} \tag{28}$$

⁵ See, for example, A. E. H. Love, *Mathematical Theory of Elasticity* (Dover Publications, Inc., New York, 1944), p. 160.

The atomic force constants may be correlated with the elastic constants by equating the elements of $E(\mathbf{q})$ to the elements of $G(\mathbf{q})$ in the long-wavelength limit, that is, by expanding $G(\mathbf{q})$ to second order in q about $\mathbf{q}=\mathbf{0}$. It is important to note that at least the first four nearest-neighbor interactions must be included in order for G to be consistent with E .

For less than four neighbors, one has the result that $(C_{12}+C_{66})=0$ which is inconsistent with the elastic data. The problem of consistency between the dynamical matrix and elastic matrix is sometimes avoided in evaluating the atomic force constants by simply equating the eigenfrequencies rather than the matrix elements. This technique can be misleading since a lack of consistency indicates that the lattice dynamics model is inadequate for the substance being studied.

Using the A-S model described in Appendix B, we obtained the following six linearly independent equations relating the atomic force constants to the elastic constants:

$$\begin{aligned}
 c(C_{12}+C_{66}) &= 8\gamma^2\delta_1K_1(4,11), \\
 c(C_{11}-C_{66}) &= 4\gamma^2\delta_2K_1(2,11)+4\gamma^2\delta_3K_1(3,12), \\
 c\gamma^2C_{44} &= 4\gamma^2\delta_1K_1(4,11)+\gamma^2\delta_2K_1(2,11) \\
 &\quad +9\gamma^2\delta_3K_1(3,12)+4C_2(4,11) \\
 &\quad + (1/2)C_2(2,11)+ (9/2)C_2(3,12) \\
 &\quad + 4C_2(1,12), \\
 c\gamma(C_{13}+C_{44}) &= 8\gamma\delta_1K_1(4,11)+2\gamma\delta_2K_1(2,11) \\
 &\quad + 18\delta_3K_1(3,12), \quad (29) \\
 cC_{44} &= 4\delta_1K_1(4,11)+\delta_2K_1(2,11)+9\delta_3K_1(3,12) \\
 &\quad + 4C_2(4,11)+C_2(2,11)+C_2(3,12), \\
 \gamma^2cC_{33} &= 4\delta_1K_1(4,11)+ (1/2)\delta_2K_1(2,11) \\
 &\quad + (81/2)\delta_3K_1(3,12)+4C_2(4,11) \\
 &\quad + (1/2)C_2(2,11)+ (9/2)C_2(3,12) \\
 &\quad + 4C_2(1,12)+4K_1(1,12).
 \end{aligned}$$

These elastic equations may be solved uniquely for the four "bond-stretching" force constants with the result that (in dyn/cm)

$$\begin{aligned}
 K_1(1,12) &= 0.92 \times 10^4, \\
 K_1(2,11) &= 1.76 \times 10^4, \\
 K_1(3,12) &= 1.28 \times 10^4, \\
 K_1(4,11) &= 0.42 \times 10^4,
 \end{aligned} \quad (30)$$

where we have used the values for the elastic constants obtained by Mason and Bömmel⁶ given in Table I.

It is interesting to note that the difference of the squares of the optical frequencies at the center of the Brillouin zone is uniquely determined by the elastic

TABLE I. Elastic and atomic force constants for white tin. Atomic force constants according to the A-S model. Elastic constants according to Mason and Bömmel.

Atomic force constants (in units of 10^4 dyn/cm)	Elastic constants (in units of 10^{11} dyn/cm ²)
$K_1(1,12) = 0.92$	$C_{11} = 7.35$
$K_1(2,11) = 1.76$	$C_{66} = 2.265$
$K_1(3,12) = 1.28$	$C_{12} = 2.34$
$K_1(4,11) = 0.42$	$C_{44} = 2.2$
$C_2(1,12) = 1.52$	$C_{13} = 2.8$
$C_2(2,11) = 0.76$	$C_{33} = 8.7$
$C_2(3,12) = -0.74$	
$C_2(4,11) = -0.20$	

constants. From Eqs. (20) and (21) it follows that

$$\begin{aligned}
 \omega_a^2 - \omega_b^2 &= (2/m)(8\gamma^2 - 4)\delta_2K_1(1,12) \\
 &\quad + (8\gamma^2 - 36)\delta_3K_1(3,12) \\
 &\simeq 0.94 \times 10^{26} \text{ rad}^2/\text{sec}^2. \quad (31)
 \end{aligned}$$

The remaining two elastic equations may be written as

$$\begin{aligned}
 4C_2(4,11) + C_2(2,11) + C_2(3,12) &= -0.77 \times 10^4, \\
 4C_2(4,11) + (1/2)C_2(2,11) + (9/2)C_2(3,12) \\
 + 4C_2(1,12) &= 2.33 \times 10^4. \quad (32)
 \end{aligned}$$

In order to determine the four atomic force constants, $C_2(s, \alpha\beta)$, two more relations are needed in addition to those of Eq. (32). We take ω_{av} as an empirical parameter so that Eq. (23) supplies an additional relation. As a final equation, we assume that

$$C_2(1,12) = tC_2(2,11), \quad (33)$$

where t is a constant factor which was expected to be on the order of unity. Thus, the atomic force constants and, consequently, the vibrational spectrum can be expressed entirely in terms of the two parameters, t , and ω_{av} . The dispersion curves, specific heat⁷ as a function of temperature from 0 to 500°K, and Debye-Waller⁸ factor at 100°K were then calculated for the range of values of t between ± 1 and ω_{av} between 1.0 and 3.0×10^{13} rad/sec. It was found empirically that the best match to the specific heat and Debye-Waller factor resulted for the values $t=0.5$ and $\omega_{av}=2.5 \times 10^{13}$ rad/sec. The atomic force constants which result from this choice are given in Table I. The value of ω_{av} obtained is in agreement with estimates that one can make from the Debye temperature for tin. For example, it is expected that the optical frequencies at $\mathbf{q}=\mathbf{0}$ should be roughly equal to the Debye frequency, $\omega_D = 2\pi k_0(\Theta_{Sn}/h)$, where k_0 and h are Boltzmann's and Planck's constant, respectively. Using the value of 189°K for the Debye temperature, Θ_{Sn} , of white tin, one obtains $\omega_{av} = 2.6 \times 10^{13}$ rad/sec.

⁷ C. A. Shiffman, Technical Report, General Electric Research Laboratory (unpublished).

⁸ J. F. Boyle, D. S. P. Bunbury, C. Edwards, and H. E. Hall, Proc. Phys. Soc. (London) 77, 129 (1961).

⁶ W. P. Mason and H. E. Bömmel, J. Acoust. Soc. Am. 28, 930 (1956).

As a second estimate we make use of the fact that the optical frequencies at the center of the Brillouin zone are approximately independent of the detailed structure of the crystal, as are the acoustical frequencies in the linear region. We have already noted that ω_{av} is independent of the a/c ratio. It is, therefore, expected that we may estimate ω_{av} on the basis of the optical frequency of germanium.⁹ Roughly, we expect

$$(\omega_{av}/\omega_{Ge}) = (\Theta_{Sn}/\Theta_{Ge}), \quad (34)$$

where ω_{Ge} is the optical frequency for germanium at the center of the zone, Θ_{Sn} is the Debye temperature for tin at room temperature, and Θ_{Ge} is the corresponding Debye temperature for germanium. Using⁹ $\omega_{Ge} = 6 \times 10^{13}$ rad/sec, $\Theta_{Sn} = 189^\circ\text{K}$, and $\Theta_{Ge} = 372^\circ\text{K}$, we find that $\omega_{av} = 3 \times 10^{13}$ rad/sec which agrees qualitatively with our previous estimate.

It is worth pointing out that if central forces are assumed and one includes the first six neighbors, then all of the force constants can be determined in terms of the elastic constants. However, such a model predicts $\omega_{av} \approx 1 \times 10^{13}$ rad/sec which is far too small.

V. NUMERICAL RESULTS AND DISCUSSION

The results of our study are summarized by the dispersion curves along the three principal symmetry directions shown in Figs. 2, 3, and 4. The atomic force constants are listed in Table I. The vibrational spectrum is characterized by low-lying optical modes, particularly near the edge of the Brillouin zone. The strong repulsion of the optical and acoustic modes results in a maximum in the longitudinal acoustic branch near the center of the zone and a flattening of all of the acoustic branches near the end of the zone. This behavior gives rise to a large density of states at intermediate acoustical frequencies and accounts for the rapid rise in the specific heat at low temperatures.

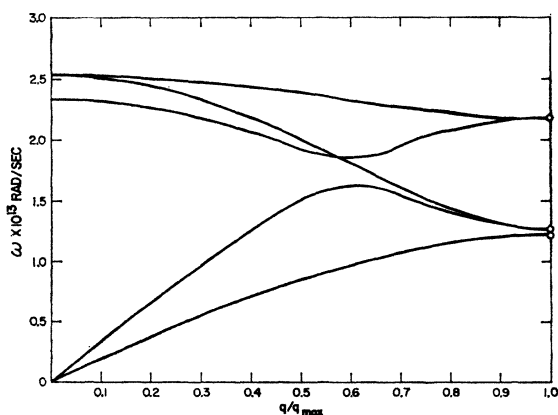


FIG. 2. Dispersion curves for white tin along [100] direction in the Brillouin zone.

⁹ B. N. Brockhouse and P. K. Iyengar, Phys. Rev. 111, 747 (1958).

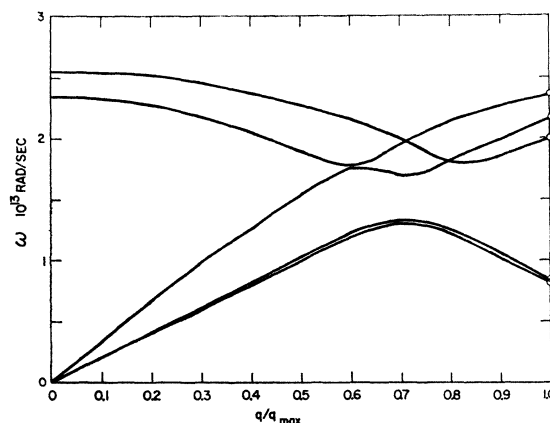


FIG. 3. Dispersion curves for white tin along the [110] direction in the Brillouin zone.

The calculated specific heat is shown in Fig. 5 and compared with experimental data. The calculated value is low from about 6°K to room temperature. It was not possible to raise the theoretical specific heat and still be consistent with other physical data. For example, the calculated specific heat can be increased by decreasing the value of ω_{av} ; however, the value of the Debye-Waller factor at 100°K then diverges rapidly from the experimental value. Furthermore, lower values of ω_{av} cause "kinks" to develop in the longitudinal acoustic branch. According to Phillips,¹ the existence of such "kinks" in an actual phonon spectrum is doubtful.

On the basis of our study it is felt that the general characteristics of the vibrational spectrum are essentially correct. There is, however, no satisfactory way of estimating the accuracy of the dispersion curves since the specific heat and Debye-Waller factor are integrated effects and not very sensitive to the parameters ω_{av} and t . Significant changes in the specific heat at low

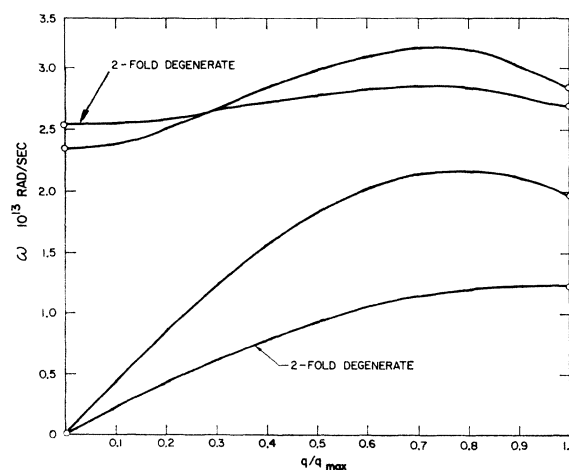


FIG. 4. Dispersion curves for white tin along [001] direction in the Brillouin zone.

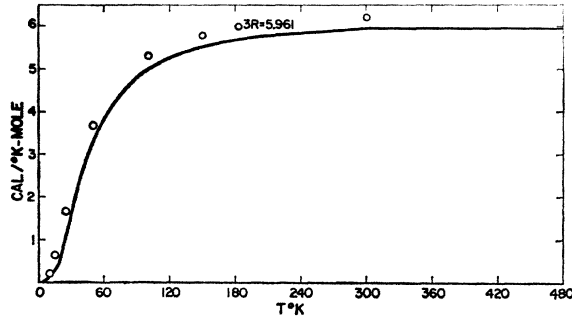


FIG. 5. Lattice specific heat for white tin. The open circles indicate the experimental values and the solid curve is the calculated theoretical specific heat. The experimental results have been corrected for the electronic contribution.

temperatures and the Debye-Waller factor resulted for changes in the parameters on the order of 10%. On the other hand, as we have seen, the general characteristics of the spectrum are essentially determined by the elastic constants.¹⁰ The detailed behavior of the acoustic and optical branches near the edge of the Brillouin zone depends upon the interaction between the two sublattices and may only be qualitatively correct.

It is clear that the tin spectrum cannot adequately be represented by a Debye approximation. It is also clear from our calculations that the optical modes contribute significantly to the specific heat at very low temperatures. At 25°K, they contributed nearly as much as the acoustic modes. The effect of the optical modes on the anisotropy in the Mössbauer Debye-Waller factor will be discussed in a subsequent paper.

APPENDIX A. STABILITY CONDITION

It is important to note that although the white tin lattice lacks a center of inversion, no requirements are imposed on the A-S atomic force constants as a result of stability considerations. To show this, let us consider the force the force, \mathbf{F}_1 , on an atom of the first sublattice in the zeroth cell due to the remainder of the crystal. According to the A-S model this force is given by

$$\mathbf{F}_1 = -\sum_{\beta} \sum_j |\mathbf{R}_j^{1\beta}|^{-2} V'(|\mathbf{R}_j^{1\beta}|) \mathbf{R}_j^{1\beta}.$$

In order to ensure the equilibrium of the lattice configuration, this force must vanish. In the absence of an inversion center it is not immediately obvious that \mathbf{F}_1 does in fact vanish for arbitrary $V'(|R|)$. We write \mathbf{F}_1 as a sum of two forces

$$\mathbf{F}_1 = \mathbf{F}(1-1) + \mathbf{F}(1-2),$$

$$\mathbf{F}(1-1) = -\sum_j |\mathbf{R}_j^{11}|^{-2} V'(|\mathbf{R}_j^{11}|) \mathbf{R}_j^{11},$$

$$\mathbf{F}(1-2) = -\sum_j |\mathbf{R}_j^{12}|^{-2} V'(|\mathbf{R}_j^{12}|) \mathbf{R}_j^{12}.$$

$\mathbf{F}(1-1)$ is the force due to sublattice one and $\mathbf{F}(1-2)$ is due to sublattice two. Each sublattice has an inversion

¹⁰ It should be mentioned that the elastic constants reported by P. W. Bridgman, Proc. Natl. Acad. Sci. U. S. 10, 411 (1924), give significantly different atomic force constants.

center and, therefore, $\mathbf{F}(1-1)$ vanishes. Furthermore, we can show that $\mathbf{F}(1-2)$ vanishes component by component. For example, the vectors \mathbf{R}_j^{12} for the first shell of neighbors are $(0, \frac{1}{2}, \frac{1}{4})$, $(0, -\frac{1}{2}, \frac{1}{4})$, $(\frac{1}{2}, 0, -\frac{1}{4})$, and $(-\frac{1}{2}, 0, -\frac{1}{4})$. Thus, the contribution to $\mathbf{F}(1-2)$ from this shell vanishes. The second shell has vectors $(\frac{1}{2}, 0, \frac{3}{4})$, $(-\frac{1}{2}, 0, \frac{3}{4})$, $(0, \frac{1}{2}, -\frac{3}{4})$, and $(0, -\frac{1}{2}, -\frac{3}{4})$ and, therefore, makes no contribution to $\mathbf{F}(1-2)$. In fact, it is easily verified that the sum of vectors of any shell vanishes. Therefore, the stability requirement for the tin lattice is automatically satisfied in the A-S model.

APPENDIX B. A-S MODEL

Within the framework of the A-S model, which has been discussed in a previous paper,³ one can write the quadratic terms in the potential energy of interaction associated with the α th atom in the zeroth unit cell as

$$V(0\alpha) = \frac{1}{2} \sum_{\beta} \sum_i |\mathbf{R}_j^{\alpha\beta}|^{-2} [C_1(j, \alpha\beta) (\mathbf{R}_j^{\alpha\beta} \cdot \Delta \mathbf{R}_j^{\alpha\beta})^2 + C_B(j, \alpha\beta) (\mathbf{R}_j^{\alpha\beta} \times \Delta \mathbf{R}_j^{\alpha\beta})^2]. \quad (\text{B1})$$

In this equation, $\mathbf{R}_j^{\alpha\beta}$ denotes a vector from the origin, chosen as the α th atom in the zeroth unit cell, to the β th atom in the j th cell. The Δ denotes a small displacement operator, $C_1(j, \alpha\beta)$ is the effective "bond-stretching" force constant for the interaction of the β th atom of the j th cell with the α th atom at the origin. Similarly, $C_B(j, \alpha\beta)$ represents an effective "bond-bending" force constant.

In the usual way, one obtains the dynamical equations for the motion of the atoms in the central cell and introduces the usual Born-von Karman cyclic boundary conditions. The vibrational spectrum is obtained by solving the determinant

$$|D(\mathbf{q}) - \omega^2 I_{3f}| = 0, \quad (\text{B2})$$

where ω is the angular frequency, \mathbf{q} is the propagation vector, and I_{3f} denotes a unit matrix of dimensions $3f$, with f being the number of atoms per unit cell. The dynamical matrix, D , may be conveniently regarded as an $f \times f$ supermatrix whose elements are 3×3 matrices. From Eq. (2), we obtain the $\alpha\beta$ th element of the supermatrix D as

$$[D(\mathbf{q})]_{\alpha\beta} = (m_{\alpha} m_{\beta})^{-1/2} \left\{ \delta_{\alpha\beta} \sum_{\sigma=1}^f A^{\alpha\sigma}(\mathbf{0}) - A^{\alpha\beta}(\mathbf{q}) \right\}, \quad (\text{B3})$$

where m_{α} is the mass of the α th type atom and $\delta_{\alpha\beta}$ is the Kronecker delta. The elements of the 3×3 matrices, $A^{\alpha\beta}(\mathbf{q})$, are given by

$$[A^{\alpha\beta}(\mathbf{q})]_{ij} = \sum_n \left\{ -|\mathbf{R}_n^{\alpha\beta}|^{-2} k_1(n, \alpha\beta) \frac{\partial^2}{\partial q_i \partial q_j} + C_B(n, \alpha\beta) \delta_{ij} \right\} \exp(i\mathbf{q} \cdot \mathbf{R}_n^{\alpha\beta}), \quad (\text{B4})$$

where

$$k_1(n, \alpha\beta) = C_1(n, \alpha\beta) - C_B(n, \alpha\beta), \quad (\text{B5})$$

The subscripts on q_i in Eq. (5) refer to the Cartesian components of \mathbf{q} . Equation (5) can also be written as

$$[A^{\alpha\beta}(\mathbf{q})]_{ij} = \sum_s \left\{ -k_1(s, \alpha\beta) \rho_s^{-2} \frac{\partial^2}{\partial q_i \partial q_j} + C_B(s, \alpha\beta) \delta_{ij} \right\} G(s, \alpha\beta), \quad (\text{B6})$$

where

$$\rho_s = |\mathbf{R}_{n(s)}^{\alpha\beta}| \quad (\text{B7})$$

is the distance between an α and β atom in the s th shell about the atom. In Eq. (7),

$$G(s, \alpha\beta) = \sum_{n(s)} \exp(i\mathbf{q} \cdot \mathbf{R}_n^{\alpha\beta}), \quad (\text{B8})$$

where the symbol $n(s)$ means that the sum is restricted to s th shell of atoms.

APPENDIX C. DYNAMICAL MATRIX FOR WHITE TIN

According to the A-S model, the matrix elements corresponding to the first four nearest-neighbor interactions can be constructed from the generators:

$$\begin{aligned} G(1, 1-1) &= 2C_{2z}, \\ G(2, 1-2) &= 2(F_z C_y + F_z^* C_x), \\ G(3, 1-2) &= 2(F_{3z} C_x + F_{3z}^* C_y), \\ G(4, 1-1) &= 8C_x C_y C_z, \end{aligned}$$

where

$$C_{nx} = \cos(nq_x a), \quad C_{ny} = \cos(nq_y a), \quad C_{nz} = \cos(nq_z c),$$

and

$$F_{nz} = \exp(incq_z/2).$$

Here, $n=1, 2$, or 3 and F^* denotes the complex conjugate of F .

From Appendix B, Eq. (B3), we find that

$$D_{11} = \begin{pmatrix} D_{xx}^{11} & D_{xy}^{11} & D_{xz}^{11} \\ D_{xy}^{11} & D_{yy}^{11} & D_{yz}^{11} \\ D_{xz}^{11} & D_{yz}^{11} & D_{zz}^{11} \end{pmatrix},$$

$$D_{12} = \begin{pmatrix} D_{xx}^{12} & D_{xy}^{12} & D_{xz}^{12} \\ D_{xy}^{12} & D_{yy}^{12} & D_{yz}^{12} \\ D_{xz}^{12} & D_{yz}^{12} & D_{zz}^{12} \end{pmatrix},$$

with

$$\begin{aligned} MD_{xx}^{11} &= MD_{yy}^{11} = 2C_2(1, 11)(1 - C_{2z}) \\ &\quad + [8T_1\gamma^2 K_1(4, 11) + 8C_2(4, 11)](1 - C_x C_y C_z) \\ &\quad + 4C_2(2, 12) + 8T_2\gamma^2 K_1(2, 12) + 8T_3\gamma^2 K_1(3, 12) \\ &\quad + 4C_2(3, 12), \end{aligned}$$

$$\begin{aligned} MD_{zz}^{11} &= [2C_2(1, 11) + 2K_1(1, 11)](1 - C_{2z}) \\ &\quad + [8C_2(4, 11) + 8T_1 K_1(4, 11)](1 - C_x C_y C_z) \\ &\quad + 4T_2 K_1(2, 12) + 4C_2(2, 12) + 36T_3 K_1(3, 12) \\ &\quad + 4C_2(3, 12), \end{aligned}$$

$$MD_{xy}^{11} = 8T_1\gamma^2 K_1(4, 11) S_x S_y C_z,$$

$$MD_{xz}^{11} = 8T_1\gamma K_1(4, 11) S_x S_z C_y,$$

$$MD_{yz}^{11} = 8T_1\gamma K_1(4, 11) S_y S_z C_x,$$

$$\begin{aligned} -MD_{xx}^{12} &= 8T_2\gamma^2 K_1(2, 12) C_x F_z^* \\ &\quad + 2C_2(2, 12)[C_y F_z + C_x F_z^*] \\ &\quad + 8T_3\gamma^2 K_1(3, 12) C_x F_{3z} \\ &\quad + 2C_2(3, 12)[C_y F_{3z}^* + C_x F_{3z}], \end{aligned}$$

$$\begin{aligned} -MD_{yy}^{12} &= 8T_2\gamma^2 K_1(2, 12) C_y F_z \\ &\quad + 2C_2(2, 12)[C_y F_z + C_x F_z^*] \\ &\quad + 8T_3\gamma^2 K_1(3, 12) C_y F_{3z}^* \\ &\quad + 2C_2(3, 12)[C_y F_{3z}^* + C_x F_{3z}], \end{aligned}$$

$$\begin{aligned} -MD_{zz}^{12} &= 2T_1 K_1(2, 12)[C_y F_z + C_x F_z^*] \\ &\quad + 2C_2(2, 12)[C_y F_z + C_x F_z^*] \\ &\quad + [18T_3 K_1(3, 12) + 2C_2(3, 12)] \\ &\quad \times (C_y F_{3z}^* + C_x F_{3z}), \end{aligned}$$

$$MD_{xy}^{12} = 0,$$

$$MD_{xz}^{12} = -i\gamma S_x [4T_2 K_1(2, 12) F_z^* - 12T_3 K_1(3, 12) F_{3z}],$$

$$MD_{yz}^{12} = +i\gamma S_y [4T_2 K_1(2, 12) F_z - 12T_3 K_1(3, 12) F_{3z}^*].$$

The S 's appearing in these equations denote sine functions whose subscripts have the same meaning as defined for the C 's. The other parameters are

$$\gamma = a/c, \quad T_1 = (1 + 2\gamma^2)^{-1}, \quad T_2 = (1 + 4\gamma^2)^{-1},$$

and

$$T_3 = (9 + 4\gamma^2)^{-1}.$$

In these equations,

$K_1(s, \alpha\beta) = C_1(s, \alpha\beta) - C_2(s, \alpha\beta)$, where $C_1(s, \alpha\beta)$ and $C_2(s, \alpha\beta)$ are, respectively, the "bond-stretching" force constant and "bond-bending" force constant for the interaction of the β th atom of the s th shell with the α th atom in the cell at the origin.

Note added in proof. Elastic constants for white tin reported by Rayne and Chandrasekhar¹¹ and by House and Vernon¹² indicate that C_{12} may be considerably higher than that obtained by Bommel and Mason.⁶ This alters the calculated vibrational spectrum significantly. In particular, the optical frequency, ω_{av} , is raised to about $1.4\omega_D$. Transverse acoustic branches along the [110] and the [001] directions are lowered, resulting in an increase in the low temperature specific heat of about 10%. The details of this calculation together with the calculations of the Debye Waller factor will be presented in a subsequent paper.

¹¹ J. A. Rayne and B. S. Chandrasekhar, Phys. Rev. **120**, 1658 (1960).

¹² D. G. House and E. V. Vernon, Brit. J. Appl. Phys. **11**, 254 (1960).